Glycyrrhizin ameliorates impaired glucose metabolism and ovarian dysfunction in a polycystic ovary syndrome mouse model

Article *in* Biology of Reproduction · April 2023

DOI: 10.1093/biolre/ioad048

CITATIONS
10

READS
284

9 authors, including:

Amin Ullah
Institutes for Systems Genetics, Frontiers Science Center for Disease-Related Mole…
26 PUBLICATIONS **219** CITATIONS

SEE PROFILE

Antonia Otoo
Chongqing Medical University
10 PUBLICATIONS **109** CITATIONS

SEE PROFILE

Enoch Adu Gyamfi Appiah
47 PUBLICATIONS **554** CITATIONS

SEE PROFILE

Biology of Reproduction, 2023, 1–14
https://doi.org/10.1093/biolre/ioad048
Research Article

Glycyrrhizin ameliorates impaired glucose metabolism and ovarian dysfunction in a polycystic ovary syndrome mouse model

Jun-Pu Yang[1], Amin Ullah[1], Ya-Nan Su[1], Antonia Otoo[1], Enoch Appiah Adu-Gyamfi[2], Qian Feng[3], Ying-Xiong Wang[1,4,*], Mei-Jiao Wang[1,4,*] and Yu-Bin Ding[1,5,6,*]

[1]Department of Obstetrics and Gynecology, Women and Children's Hospital of Chongqing Medical University, Chongqing, China
[2]Department of Genetics, Development and Cell Biology, Iowa State University, Ames, IA, USA
[3]Department of Obstetrics and Gynecology, Chongqing Hospital of Traditional Chinese Medicine, Chongqing, China
[4]Department of Physiology, School of Basic Medical Science, Chongqing Medical University, Chongqing, China
[5]Department of Toxicology, School of Public Health, Chongqing Medical University, Chongqing, China
[6]Department of Pharmacology, Academician Workstation, Changsha Medical University, Changsha, China

***Correspondence**: Department of Obstetrics and Gynecology, Women and Children's Hospital of Chongqing Medical University, No. 120 Longshan Road, Yubei District, Chongqing 401147, China. Tel: +8602368485008; Fax: +8602368485000; E-mail: dingyb@cqmu.edu.cn, yxwang@cqmu.edu.cn, meijiaowang@cqmu.edu.cn

[†]**Grant Support**: This work was funded by grants from the National Natural Science of Foundation of China (Nos. 81971391, 82271707, 82171624), Natural Science of Foundation of Chongqing (Nos. cstc2021jcyj-msxmX0236, cstc2021jcyj-msxmX0900, cstc2020jcyj-msxmX0294), and Joint project of Chongqing Health Commission and Science and Technology (No. 2022QNXM042).

Abstract

The aim of this study was to determine the impact of glycyrrhizin, an inhibitor of high mobility group box 1, on glucose metabolic disorders and ovarian dysfunction in mice with polycystic ovary syndrome. We generated a polycystic ovary syndrome mouse model by using dehydroepiandrosterone plus high-fat diet. Glycyrrhizin (100 mg/kg) was intraperitoneally injected into the polycystic ovary syndrome mice and the effects on body weight, glucose tolerance, insulin sensitivity, estrous cycle, hormone profiles, ovarian pathology, glucolipid metabolism, and some molecular mechanisms were investigated. Increased number of cystic follicles, hormonal disorders, impaired glucose tolerance, and decreased insulin sensitivity in the polycystic ovary syndrome mice were reverted by glycyrrhizin. The increased high mobility group box 1 levels in the serum and ovarian tissues of the polycystic ovary syndrome mice were also reduced by glycyrrhizin. Furthermore, increased expressions of toll-like receptor 9, myeloid differentiation factor 88, and nuclear factor kappa B as well as reduced expressions of insulin receptor, phosphorylated protein kinase B, and glucose transporter type 4 were restored by glycyrrhizin in the polycystic ovary syndrome mice. Glycyrrhizin could suppress the polycystic ovary syndrome-induced upregulation of high mobility group box 1, several inflammatory marker genes, and the toll-like receptor 9/myeloid differentiation factor 88/nuclear factor kappa B pathways, while inhibiting the insulin receptor/phosphorylated protein kinase B/glucose transporter type 4 pathways. Hence, glycyrrhizin is a promising therapeutic agent against polycystic ovary syndrome.

Summary Sentence

Glycyrrhizin could improve inflammation, glucose metabolic disorders, and ovarian dysfunction in polycystic ovary syndrome mice by inhibiting the expression of high mobility group box 1.

Keywords: polycystic ovary syndrome, glycyrrhizin, high mobility group box 1, insulin resistance, ovarian dysfunction

Introduction

Polycystic ovary syndrome (PCOS) is a continuous reproductive and metabolic disorder that affects, at least, 17% of childbearing-age women worldwide [1]. Hyperandrogenism, anovulation, and polycystic ovarian morphology are the most prominent characteristics of PCOS [2]. Apart from hormonal disorders, obesity, and insulin resistance (IR) [3, 4], low-grade chronic inflammation often accompanies PCOS [5]. Hence, PCOS patients have a higher risk of developing metabolic syndrome, type 2 diabetes, and cardiovascular diseases in the future [6].

IR is the most common metabolic disorder in PCOS patients, having a prevalence of 65–70% among these patients [7], especially in the patients with obesity [8]. Compensatory hyperinsulinemia causes androgen-dependent anovulation, leading to reproductive defects in PCOS patients [9]. In addition, women with PCOS and obesity exhibit marked adipose tissue dysfunction and dysregulated adipokine secretion, which result in a chronic pro-inflammatory state [10, 11]. Infiltrating inflammatory cells trigger insulin resistance, stimulate androgen secretion, and further disrupt the function of the hypothalamic–pituitary–ovarian axis [12, 13], resulting in ovarian dysfunction in PCOS. An association between high mobility group box 1 (HMGB1) and IR in PCOS has been found [14], but the pathogenesis of PCOS is still not clear.

Received: October 14, 2022. **Revised:** March 24, 2023. **Accepted:** April 21, 2023

HMGB1 is a highly conserved protein [15]. It is released from cells in a noncanonical pattern and thought to be a fatal late inflammatory factor [16, 17]. Several studies have demonstrated that the serum and follicular fluid levels of HMGB1 are higher in PCOS patients [18], which indicates that HMGB1 is possibly involved in the pathophysiology of PCOS. Moreover, by silencing HMGB1, endocrine disturbances, proliferation, and apoptosis of ovarian granulosa cells could be inhibited significantly [19]. This indicates that HMGB1 inhibitors might be potent drugs to treat PCOS. Glycyrrhizin, a naturally occurring compound from the licorice plant, can directly bind to and inhibit HMGB1 [20]. Although glycyrrhizin has shown potential benefits in the treatment of inflammation and obesity [21, 22], its therapeutic effects against PCOS has not been explored.

Thus, in this study, we aimed to find out whether glycyrrhizin could reverse the metabolic and reproductive disorders in PCOS through inhibiting HMGB1. To achieve this, we treated PCOS mice with glycyrrhizin and then assessed its therapeutic effects on the mice. Our findings point to the possible utilization of glycyrrhizin in the treatment of PCOS.

Materials and methods

Experimental animals

This animal study was performed according to the guidelines and protocols of the Institutional Animal Care and Use Committee of Chongqing Medical University (Approval No. 2022108). A total of 120 female C57BL/6J mice (21 days; weight 7–9 g) were purchased from the Animal Research Center of Chongqing Medical University. The mice were housed at a controlled temperature of 24 ± 2°C in standard cages with 55 ± 15% humidity and a 12 h light/dark cycle. The mice had free access to water and food, and were allowed to acclimatize to their new environment for a period of 4 days before experimentation.

Treatment scheme

Figure 1A shows the conceptual model of the study. Twenty-five-day-old female prepuberal C57BL/6J mice were randomly divided into four groups ($n = 30$ per group): control, PCOS, PCOS plus glycyrrhizin, and PCOS plus vehicle. The control mice were injected daily with 0.1 mL of sesame oil (241002500; Acros Organics, Belgium) and fed with a normal diet composed of standard chow. To induce PCOS [23–25], we subcutaneously injected the mice with 6 mg/100 g dehydroepiandrosterone (DHEA, 252805; EMD Milliporep, MA, USA) dissolved in DMSO (D2650-100ML; Sigma-Aldrich, USA) and 0.1 mL sesame oil and then fed them with a high-fat diet (HFD, 60% kcal fat; Hua Fu Kang, Beijing, China). The PCOS plus glycyrrhizin group received 100 mg/kg glycyrrhizin (53956-04-0, Sigma-Aldrich, MO, USA; dissolved in 0.1 mL of saline) intraperitoneally on each day [26, 27], while the PCOS plus vehicle group mice were injected with 0.1 mL saline intraperitoneally. The body weights of the mice were monitored every 4 days.

Collection of blood, ovaries, and uteri and determination of body mass index

Blood was collected through myocardial puncture and then centrifuged at $1000 \times g$ for 20 min at 4°C to obtain serum. The left ovary of each mouse was collected for histological analysis. The right ovary was kept at −80°C for RNA and protein extraction. The uterus of each mouse was removed and its weight recorded. The body length of each mouse was measured from the nose to the anus [28]. Body mass index (BMI) was calculated by using the formula [(body weight)/length^2].

Estrous cycle determination

Estrous cycle was daily determined from the 11th day via vaginal smear analysis. Vaginal cells were collected, fixed with 4% paraformaldehyde, and stained with methylene blue (G1302; Solarbio Life Science, Beijing, China). Stages of the estrous cycle were determined based on vaginal cytology, and the corresponding images are shown in Figure S1.

Oral glucose tolerance test, insulin tolerance test, and glucose metabolism indexes assessment

After the mice had fasted for 6 h, we measured their fasting blood glucose from their tail veins. Ten mice were randomly selected and given glucose (2 g/kg body weight) via oral gavage for oral glucose tolerance test (OGTT) [29]. Then, another batch of 10 mice were injected intraperitoneally with insulin (0.75 IU/kg body weight) for insulin tolerance test (ITT) [30]. The blood glucose levels were measured at 15, 30, 60, 90, and 120 min post-treatment by using an ACCU-CHEK glucometer (Roche, Ireland). Mouse insulin enzyme-linked immunosorbent assay (ELISA) kit (JL11459; J&L Biological, Shanghai, China) was used to test serum insulin level. The intra- and inter-assay errors were <9% and <11%, respectively. Limits of sensitivity were 0.1 mIU/L. The homeostatic model assessment of IR (HOMA-IR) and beta cell function (HOMA-β) indexes were calculated with the formula: [FG (mmol/L)] × [FINS (IU/mL)]/22.5 and [20 × FINS (IU/mL)]/[FG (mmol/L) − 3.5].

Analysis of serum hormone concentrations

Serum testosterone, luteinizing hormone (LH), and follicle-stimulating hormone (FSH) levels were determined using ELISA kits (JL25196, JL10432, and JL10239; J&L Biological). Intra- and inter-assay errors were <9% and <11%, respectively. The sensitivity limit of testosterone was 0.1 ng/mL, and that of LH and FSH were 0.1 mIU/mL.

Serum lipid profile measurement

Serum high-density lipoprotein cholesterol (HDL-C), low-density lipoprotein cholesterol (LDL-C), total cholesterol (TC), and triglyceride were measured using commercially available colorimetric diagnostic kits (A112-1-1, A113-1-1, A111-1-1, and A110-1-1; Nanjing Jian Cheng Bioengineering Institute, Nanjing, China).

Serum HMGB1 ELISA

Serum HMGB1 concentration was measured with an ELISA kit (JL13702; J&L Biological). For sensitivity, the minimum detection concentration was less than 0.1 ng/mL while the detection range was from 0.625 to 20 ng/mL. The intra-assay and inter-assay errors were less than 9% and 11%, respectively.

Tissue processing and histological staining

Each group's ovaries were randomly sampled, fixed with 4% paraformaldehyde, embedded in paraffin, and cut into

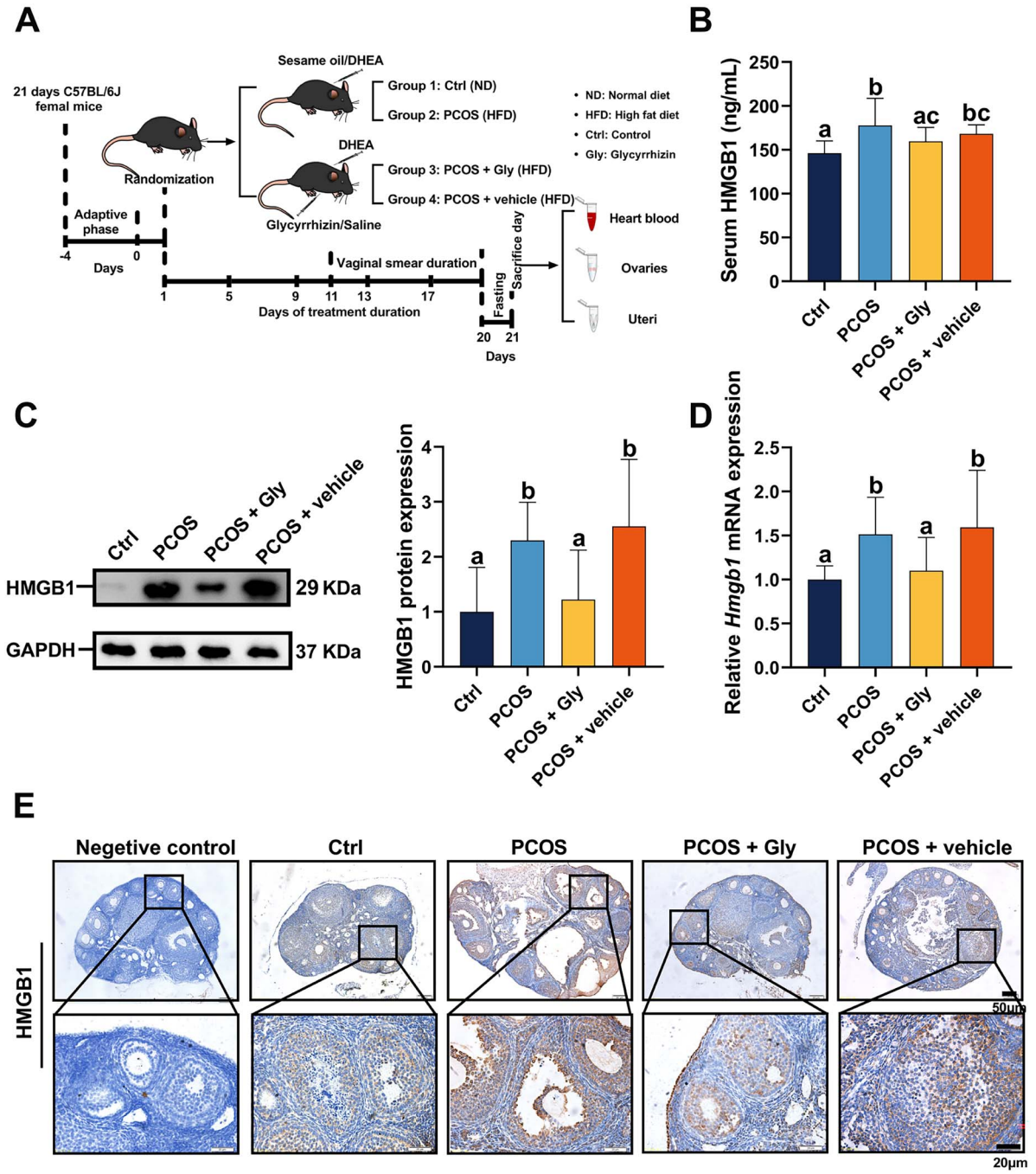

Figure 1. Effect of glycyrrhizin on HMGB1 expression in PCOS mice. (A) The group assignments and timeline of the experimental procedure; (B) serum HMGB1 level, $n = 10$–21 per group; (C) HMGB1 protein levels in the mice ovary, $n = 12$ per group; (D) RT-qPCR analysis of *Hmgb1* mRNA levels in the mice ovary, $n = 11$–17 per group; (E) immunohistochemical images of HMGB1 expression in ovarian tissues. Bars = 50 μm, 20 μm. Data are presented as mean ± SD; different lowercase letters above the columns, such as a, b, and c, indicate $P < 0.05$. If two columns have the same lowercase letter, it indicates no statistical significance. HMGB1, high mobility group box 1.

5 μm sections. Six sections from each ovary were stained with hematoxylin and eosin (H&E) for histological analysis and follicle counting [31, 32].

Immunohistochemical staining

Immunohistochemical (IHC) staining was performed by using a kit (SP-9001; ZSGB-BIO, Beijing, China). Antigen were retrieved with sodium citrate buffer (pH 6.0, ZLI-9064; ZSGB-BIO). Mouse ovarian sections were incubated overnight at 4°C with the antibodies of HMGB1 (1:100, D260488; Sangon Biotech, Shanghai, China), toll-like receptor (TLR) 9 (1:200, bs-23640R; Bioss, Beijing, China), and nuclear factor kappa B (NF-κB, 1:200, bs-0465R; Bioss). The visualization of the immune complexes was carried out using the DAB kit (ZLI-9018; ZSGB-BIO).

KGN cell experiments

Human granulosa cell-like tumor cell line (KGN; Suer, Shanghai, China), characterized by functional FSH receptors and other similarities with in vivo ovarian granulosa cells, is

commonly used to study the function and underlying mechanism of granulosa cells in PCOS [33–35]. Here, KGN cells were cultured in DMEM/F12 (D6429; Sigma) supplemented with 15% fetal bovine serum (20180918; Kang Yuan Biology, Tianjin, China), 100 U/mL penicillin G, and 0.1 mg/mL streptomycin sulfate (C0224; Beyotime, Shanghai, China) in a humidified atmosphere with 5% CO_2 at 37°C. In the glycyrrhizin treatment group, the glycyrrhizin was mixed with phosphate buffered saline and then diluted into 15 mM by using complete medium.

Cell counting kit-8 assay

KGN cells were seeded in 96-well plates at 2×10^3 cells/well and cultured for 24 h. The cells were then treated with glycyrrhizin at different concentrations for 24 h, 48 h, and 72 h. The viability of KGN cells was detected by using the cell counting kit-8 (CCK-8) assay. The CCK-8 reagent (1:10, C0005; TargetMol, Shanghai, China) was put into each well and incubated for 2 h. The absorbance was read at 450 nm by using a microplate reader (SpectraMax iD5, Beijing, China). To determine the optimal glycyrrhizin concentrations and treatment duration, we treated HMGB1-overexpression cells with 0, 0.5, 1, 2, 5, 7.5, 10, and 15 mM of glycyrrhizin for 24 h, 48 h, and 72 h. Finally, 2 mM glycyrrhizin concentration and 24 h treatment duration were chosen for further study since the cell viability was minimally affected under these conditions.

Cell transfection

The KGN cells were grown in a 6-well cell culture plate (9.5 cm^2) and allocated to the following groups: control (CD513B plasmid), OE-HMGB1 (HMGB1 overexpression plasmid), OE-HMGB1 + Gly (HMGB1 overexpression plasmid plus glycyrrhizin), and OE-HMGB1 + vehicle (HMGB1 overexpression plasmid plus phosphate buffer saline) groups. Lipo8000 was used as the transfection reagent (C0533; Beyotime). The transfection duration was 48 h, while the glycyrrhizin-treatment duration was 24 h. Transfection efficiency was evaluated with real-time quantitative polymerase chain reaction (RT-qPCR) and western blot analysis at 48 h post-transfection.

A commercially synthesized HMGB1-specific small interfering RNA (siRNA; Genepharma, Shanghai, China) was used for HMGB1 silencing. The HMGB1 siRNA sequences were as follows: si-HMGB1#1, 5′-GCAUAAGAAGAAGCACCCATT-3′; si-HMGB1#2, 5′-GGACAAGGCCCGUUAUGAATT-3′; si-HMGB1#3, 5′-GCAGAU GACAAGCAGCCUUTT-3′. Cells were allocated to the following groups: mock (untransfected cells); si-NC (scrambled siRNA); si-HMGB1#1, #2, and #3 (cells transfected with three HMGB1 siRNA recombinant plasmids, respectively). Lipo8000 was used as the transfection reagent. Transfection efficiency was evaluated with RT-qPCR at 48 h post-transfection and with western blot analysis at 72 h post-transfection. si-HMGB1#2 was then selected for further study since it elicited the highest silencing efficiency.

Real-time quantitative polymerasechain reaction

Total RNA was extracted by using Trizol (#9108; Takara Biomedical Technology, Beijing, China) and transcribed using RT mix (0000418224; Eastep, Beijing, China). RT-qPCR was performed using SYBR (#C0006; TargetMol). The mice mRNA expression relative to beta actin (*Actb*) and the cells' mRNA relative to glyceraldehyde-3-phosphate dehydrogenase (*Gapdh*) were determined using the $2^{-\Delta\Delta}$ cq method, normalized and presented as fold-change compared to the control group. The primer sequences are shown in Table S1.

Western blot

Protein was extracted using RIPA lysis buffer (P0013B; Beyotime). Primary antibodies specific to GAPDH (1:1000, AB-P-R001; GOODHERE, Zhejiang, China), HMGB1 (1:1000, #6893; Cell Signaling Technology, USA), TLR4 (1:1000, bs-20594R; Bioss), TLR9 (1:1000; Bioss), glucose transporter type 4 (GLUT4, 1:1000, #2213S; Cell Signaling Technology), total-AKT (t-AKT, 1:1000, #4691; Cell Signaling Technology), phosphorylated-AKT (p-AKT, 1:1000, #4060; Cell Signaling Technology), and NF-κB (1:1000; Bioss) were incubated overnight at 4°C. Membranes were probed with horseradish peroxidase-conjugated secondary antibody (1:5000, #abs20039ss and #abs20040ss; Absin Bioscience, Shanghai, China). Signals were detected with the ECL reagent (Cat. No. P10300; New Cell & Molecular Biotech, Shanghai, China). Band intensities were measured using the ImageJ software (version 1.53e; Wayne Rasband and contributors of National Institute of Health, USA).

Data and statistical analysis

All values are presented as mean ± standard deviation (SD) of at least triple tests. Differences between two groups were analyzed by using a two-tailed unpaired Student *t*-test coupled with Welch correction. Multigroup comparisons were analyzed using one-way or two-way analysis of variance followed by Tukey multiple comparisons test. The association between the levels of serum HMGB1 and other related biomarkers was determined with Pearson correlation coefficient. GraphPad Prism (version 9.4.1; GraphPad Software, CA, USA) was conducted for statistical analysis. $P < 0.05$ was used to indicate significant difference between/among groups.

Results

Glycyrrhizin reduced HMGB1 expression in PCOS mice

To demonstrate the effect of glycyrrhizin on HMGB1 expression, we first assessed the serum levels as well as the mRNA and protein levels of HMGB1 in the ovaries of each group. The level of serum HMGB1 in the PCOS mice was higher than that in the controls ($P < 0.01$). This level decreased significantly after glycyrrhizin treatment ($P < 0.05$; Figure 1B) although no significant change was found in the PCOS plus vehicle group (Figure 1B). HMGB1 protein and mRNA levels in the PCOS mice ovaries were significantly higher than those in the control group ($P < 0.01$), and reduced by glycyrrhizin ($P < 0.05$; Figure 1C and D). IHC staining showed that HMGB1 is expressed in the granulosa cells, theca cells, and oocytes, with higher levels in the PCOS mice than in the controls. Glycyrrhizin reduced HMGB1 expression in the PCOS mice (Figure 1E). Together, these data demonstrate that glycyrrhizin inhibits HMGB1 in PCOS mice.

Glycyrrhizin failed to alleviate the increased body weight of PCOS mice

To clarify the effect of glycyrrhizin on PCOS mice, we recorded their body weight, ovarian weight, and uterine

phenotypes. The results of the area under the body weight curve (AUC) indicate that the PCOS mice had higher body weights than the controls ($P < 0.05$, Figure 2A), but when comparing the PCOS + Gly group with PCOS + vehicle group, there was no significant difference. The PCOS mice had higher BMI than the control mice ($P < 0.01$), but glycyrrhizin was able to decrease it slightly (Figure 2B). The wet ovarian weight of the PCOS mice was significantly higher than that of the control mice ($P < 0.05$). However, it decreased after glycyrrhizin treatment slightly (Figure 2C). The wet weight of the uteri of the PCOS mice was significantly higher than that of the control group ($P < 0.001$, Figure 2D–F). Besides, glycyrrhizin significantly decreased it in the PCOS mice ($P < 0.05$; Figure 2D). Taken together, our data show that glycyrrhizin was not able to reduce the weight gain of the PCOS mice to a certain extent, but it effectively reduced the swollen uteri of the PCOS mice.

Glycyrrhizin treatment ameliorated glucolipid metabolism in the PCOS mice while an increased HMGB1 correlated with HOMA-IR, HOMA-β, and LDL-C

To further explore the effect of glycyrrhizin on PCOS, we measured glucose and lipid metabolism indexes. Fasting glucose and fasting serum insulin levels were increased in the PCOS mice as compared with the controls ($P < 0.05$; Figure 3A and B). The fasting serum insulin level was significantly decreased by glycyrrhizin ($P < 0.001$; Figure 3B). The HOMA-IR value was higher in the PCOS mice than in the controls ($P < 0.05$) but was decreased after treatment with glycyrrhizin ($P < 0.001$; Figure 3C). HOMA-β index was increased after glycyrrhizin administration in the PCOS mice ($P < 0.05$; Figure 3D). The OGTT assay revealed a delayed glucose tolerance and increased AUC in the PCOS mice than in the controls ($P < 0.001$). This glucose tolerance impairment was alleviated by glycyrrhizin ($P < 0.05$; Figure 3E). During the ITT assay, we observed that after insulin treatment, blood glucose level decreased more slowly and had a higher AUC value in the PCOS mice than in the controls ($P < 0.005$). Glycyrrhizin, but not the vehicle, significantly attenuated insulin resistance in the PCOS mice ($P < 0.05$; Figure 3F). The PCOS mice exhibited significantly higher serum TC, LDL-C, and HDL-C levels than the controls ($P < 0.001$, $P < 0.001$, and $P < 0.01$; Figure S2A–D). LDL-C level was markedly decreased in the PCOS mice following glycyrrhizin administration ($P < 0.05$; Figure S2C).

Furthermore, with the increase of serum HMGB1 level, fasting glucose and insulin levels showed an increasing trend (Figure 3G and H). HMOA-IR and serum HMGB1 levels correlated positively ($r = 0.646$, $P = 0.0095$; Figure 3I), while HOMA-β and serum HMGB1 levels correlated negatively ($r = 0.4876$, $P = 0.0292$; Figure 3J). Serum HMGB1 correlated positively with LDL-C ($r = 0.6376$, $P = 0.0025$; Figure S2G). Taken together, our data indicate that glycyrrhizin corrects impaired glucose tolerance and insulin insensitivity. It also partially corrects lipid metabolic disorders.

Glycyrrhizin reduced the expression of inflammatory factors via HMGB1 inhibition

Due to the increased ovarian weights and swollen uteri in the PCOS mice, we suspected that HMGB1 might be related to inflammation. So, we tested some important inflammatory factors in HMGB1-silenced KGN cells. HMGB1 knockdown significantly decreased the mRNA levels of *Il6*, *Tnfα*, and *Ifnβ* ($P < 0.001$, $P < 0.01$, and $P < 0.001$, respectively). The mRNA levels of *Il1β*, *Ifnα*, and *Ifnγ* decreased slightly but the changes were not significantly different (Figure 4A–F).

RT-qPCR results showed that *Tnfa*, *Ifna*, and *Ifnb1* mRNA levels were significantly increased in the PCOS mice ovaries when compared with those of the controls ($P < 0.05$) but were significantly reduced by glycyrrhizin ($P < 0.05$; Figure 4H, J, and K). Also, the drug was able to reduce *Il6* and *Ifng* mRNA levels in the PCOS mice ($P < 0.05$; Figure 4G and L).

In addition, glycyrrhizin was used to treat the KGN cells. RT-qPCR results showed that glycyrrhizin significantly reduced the expressions of *Il6*, *Tnfa*, *Ifna*, and *Ifnb1* ($P < 0.05$; Figure 4M, N, P and Q). The mRNAs of *Il1b* and *Ifng* also showed similar changes, but the differences were not significant (Figure 4O and R).

Glycyrrhizin partly reversed ovarian function disorders in the PCOS mice

In view of the effects of glycyrrhizin on glucolipid metabolism and inflammation in PCOS mice, we further explored the effects of glycyrrhizin on ovarian function in PCOS mice. Compared with the control group, the PCOS mice exhibited complete loss of estrous cyclicity (Figure 5A and B), as well as increased cyst-like follicles and reduced number of the corpus lutea ($P < 0.001$; Figure 5C and D). Surprisingly, glycyrrhizin treatment prolonged the metestrus phase (Figure 5A and B) and decreased the number of cystic follicles but increased the primordial follicles, primary follicles, and corpus lutea formation in the PCOS mice ($P < 0.01$; Figure 5C and D).

The serum testosterone level was higher in the PCOS mice than in the controls ($P < 0.05$) but was reduced after treatment with glycyrrhizin ($P < 0.01$; Figure 5E). Elevated serum LH in the PCOS mice was significantly alleviated by glycyrrhizin ($P < 0.05$; Figure 5F). There was no difference in serum FSH level among the four groups (Figure 5G). Serum LH/FSH ratio was increased in the PCOS mice compared with the control mice ($P < 0.05$) and could be alleviated by glycyrrhizin ($P < 0.05$; Figure 5H).

Moreover, correlation analysis showed that serum testosterone, LH, FSH, and LH/FSH ratios tended to associate with the increase in HMGB1 level (Figure 5I–L). Particularly, there was a significant positive correlation between serum testosterone and HMGB1 levels ($r = 0.5406$, $P = 0.0036$; Figure 5I), suggesting that HMGB1 is related to hormone levels. Taken together, our data suggest that glycyrrhizin can partially reverse ovarian dysfunction in PCOS by inhibiting HMGB1.

HMGB1 led to inflammatory cascade amplification, possibly through the HMGB1–TLR9–MyD88–NF-κB pathway

TLR4 and TLR9 are important receptors of HMGB1 [36], which may play a role in PCOS women [37]. Myeloid differentiation primary response protein 88 (MYD88) is a general adaptor protein that acts downstream of the TLRs to mediate NF-κB activation [38]. The results showed that protein levels of TLR4, TLR9, and NF-κB in the PCOS mice were significantly higher than those in the controls, but glycyrrhizin administration decreased their levels (all $P < 0.05$ respectively;

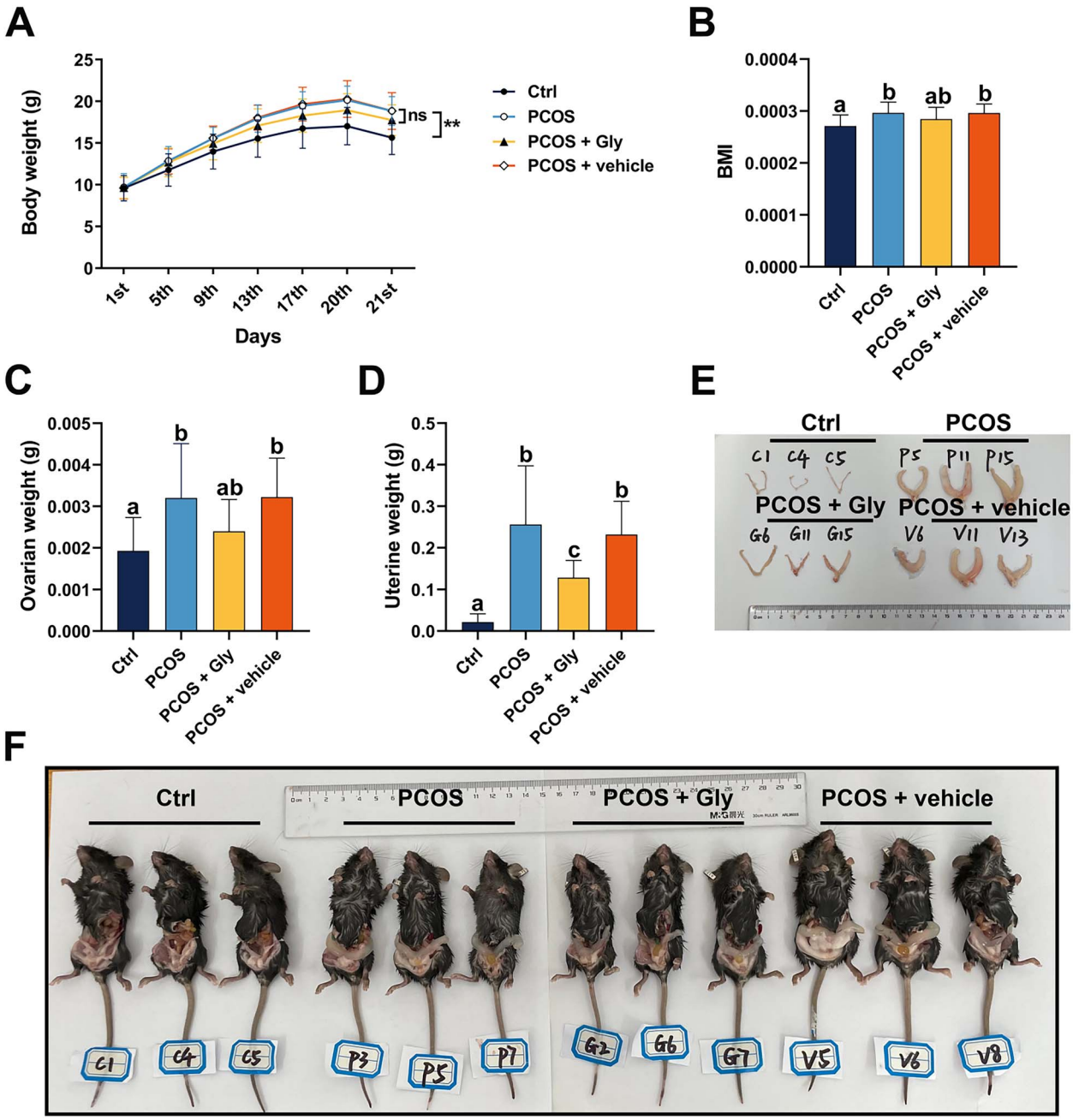

Figure 2. Effect of glycyrrhizin on body weights and ovarian and uterine weights in PCOS mice. (A) Average body weight curves for each group of mice, $n = 15$ per group. (B) BMI and (C) ovarian weights, $n = 9$–14 per group. (D) The wet weight of the uteri, $n = 9$–15 per group. (E, F) Uterine phenotype of each mouse group, $n = 3$ per group. Data are presented as mean ± SD. Different lowercase letters above the columns, such as a, b, and c, indicate $P < 0.05$. If two columns have the same lowercase letter, it indicates no statistical significance; $^{**}P < 0.01$, control vs. PCOS. BMI, body mass index.

Figure 6A and B). The mRNA levels of *Tlr4*, *Tlr9*, *Myd88*, and *Nfκb* showed the same trend as the proteins ($P < 0.05$; Figure 6C). IHC staining showed that TLR9 and NF-κB levels in the PCOS and PCOS + vehicle groups were increased when compared with those of the control and PCOS + glycyrrhizin groups ($P < 0.05$, Figure 6D and E). TLR9 was widely expressed in the cytoplasm of all developing follicles and oocytes. NF-κB was mainly expressed in the cytoplasm of all developing follicles, oocytes, and granulosa cells.

HMGB1 levels were significantly increased at both protein and mRNA levels in the KGN cells that were transfected with the HMGB1-overexpression plasmid ($P < 0.05$, Figure 6F–H). CCK-8 results showed that treatment of the KGN cells with 5 mM or higher concentrations of glycyrrhizin for 24 h produced a significant inhibitory effect on cell viability ($P < 0.001$, Figure 6I). Twenty-four-hour treatment with glycyrrhizin did not show significant differences among 0 mM, 1 mM, and 2 mM (Figure 6J). The protein levels of HMGB1, TLR4, TLR9, and NF-κB in the HMGB1 overexpression group were significantly reduced by glycyrrhizin administration (all $P < 0.05$; Figure 6K and L). The mRNA levels of *Hmgb1*, *Tlr4*, *Tlr9*, *Myd88*, and *Nfκb* showed the same trend as the proteins ($P < 0.05$; Figure 6M).

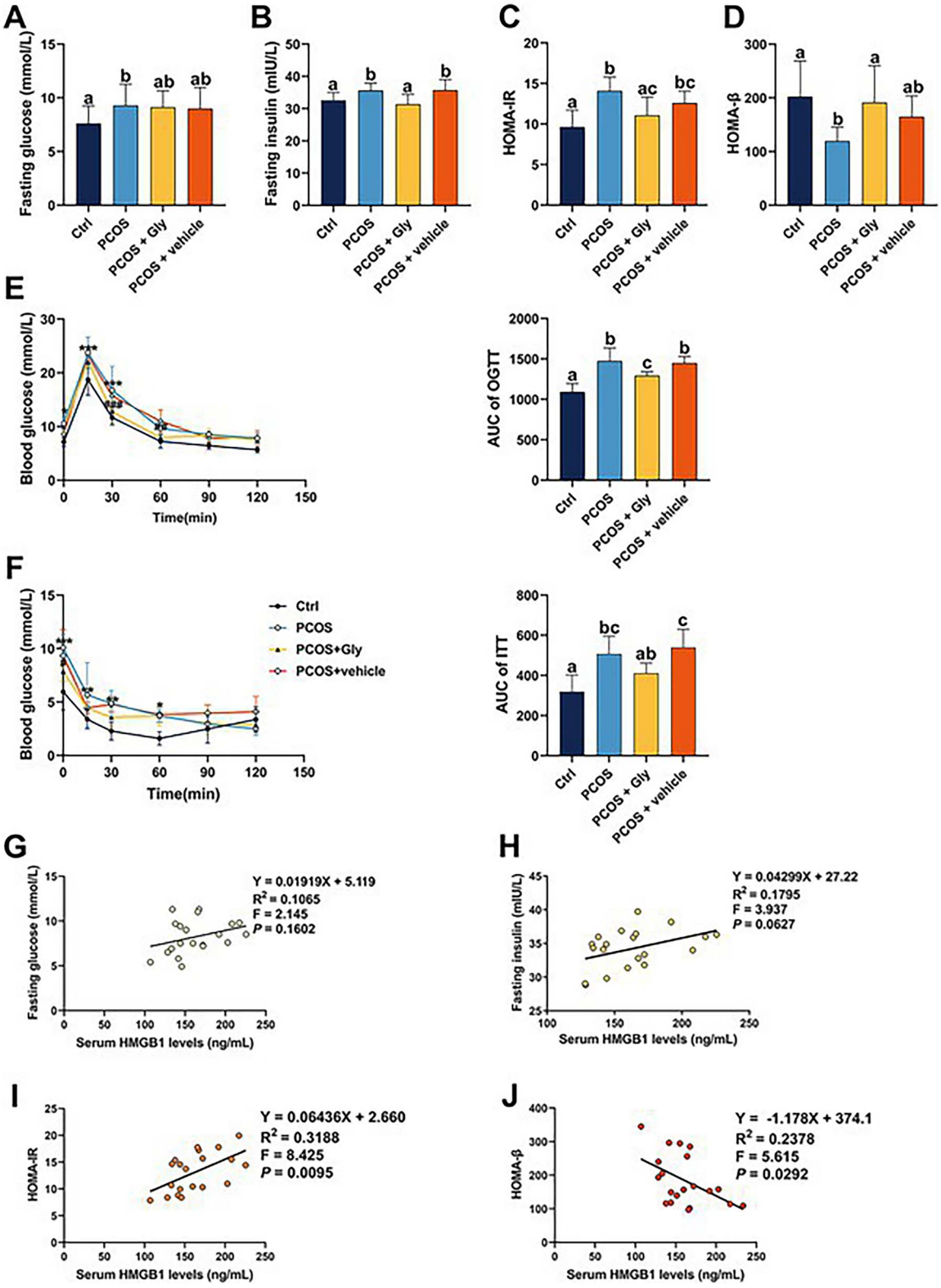

Figure 3. Changes in the glucose metabolic disorders in mice with PCOS administered with glycyrrhizin. (A) Blood glucose, (B) serum insulin levels, (C) HOMA-IR, and (D) HOMA-β of the four groups of mice, $n = 11$–20 per group. (E) OGTT ($n = 7$ per group) and (F) ITT ($n = 7$ per group) and corresponding AUCs. Correlation between serum HMGB1 level and (G) fasting glucose, (H) fasting insulin, (I) HOMA-IR, and (J) HOMA-β ($n = 20$). Data are presented as mean ± SD. Different lowercase letters above the columns, such as a, b, and c, indicate $P < 0.05$. If two columns have the same lowercase letter, it indicates no statistical significance; $^{*}P < 0.05$, control vs. PCOS; $^{**}P < 0.01$, control vs. PCOS; $^{***}P < 0.001$, control vs. PCOS; $\#P < 0.05$, PCOS + Gly vs. PCOS + vehicle; $\#\#P < 0.01$, PCOS + Gly vs. PCOS + vehicle; $\#\#\#P < 0.001$, PCOS + Gly vs. PCOS + vehicle; OGTT, oral glucose tolerance test; ITT, insulin tolerance test; AUC, area under the curve.

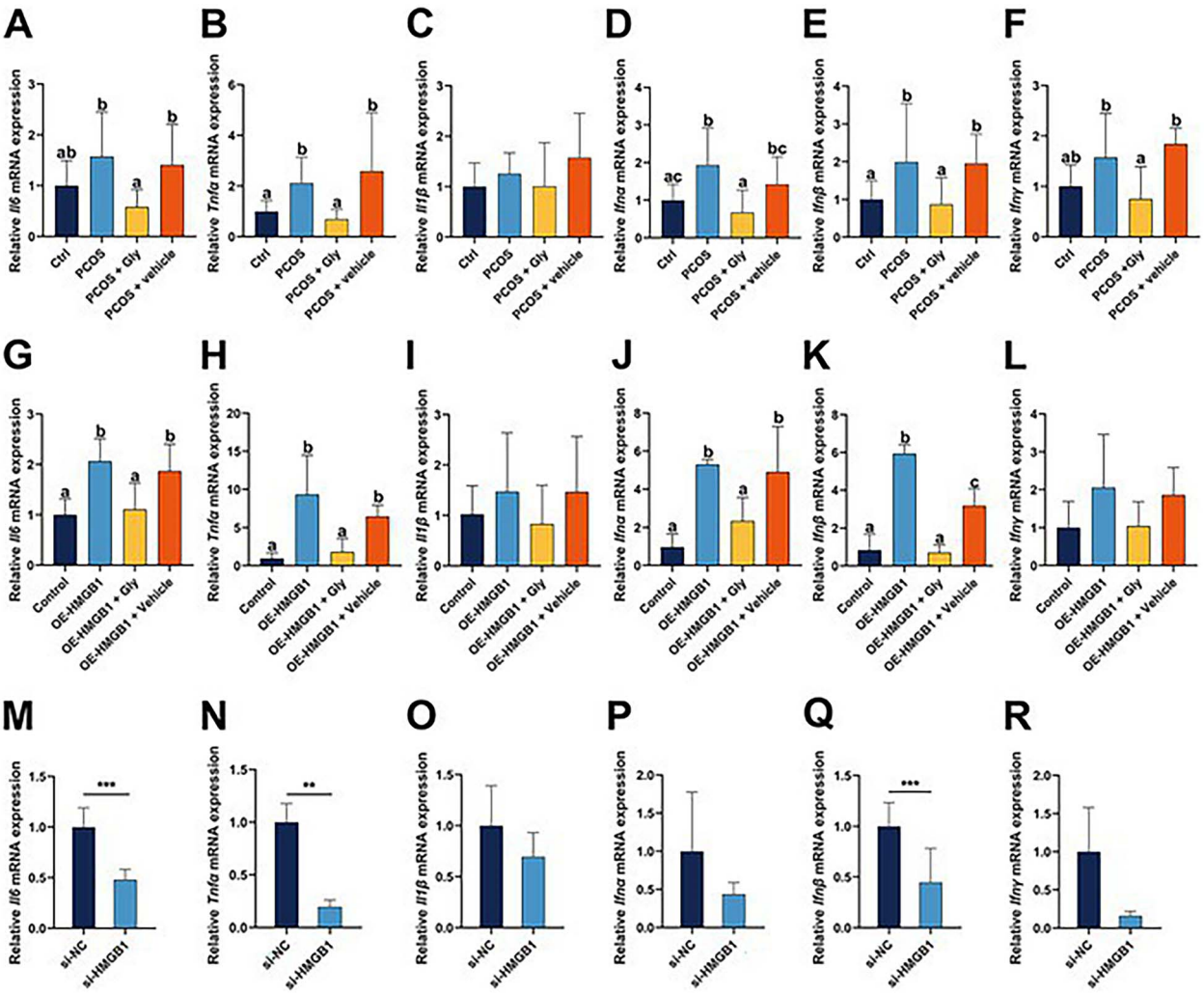

Figure 4. mRNA expression of inflammatory factors after inhibiting HMGB1 by qPCR analysis both in vivo and in vitro. Ovarian mRNA levels of (A) *Il6*, (B) *Tnfa*, (C) *Il1b*, (D) *Ifna*, (E) *Ifn1*, and (F) *Ifng* in the mice ($n = 10$–12 per group). The mRNA levels of (G) *Il6*, (H) *Tnfa*, (I) *Il1b*, (J) *Ifna*, (K) *Ifnb1*, and (L) *Ifng* in KGN cells with HMGB1 overexpression ($n = 9$ per group). The mRNA levels of (M) *Il6*, (N) *Tnfa*, (O) *Il1b*, (P) *Ifna*, (Q) *Ifnb1*, and (R) *Ifng* in KGN cells with HMGB1 knockdown ($n = 9$ per group). The data are expressed as mean ± SD. Different lowercase letters above the columns, such as a, b, and c, indicate $P < 0.05$. If two columns have the same lowercase letter, it indicates no statistical significance; $^{*}P < 0.05$, si-NC vs. si-HMGB1; $^{**}P < 0.01$, si-NC vs. si-HMGB1; $^{***}P < 0.001$, si-NC vs. si-HMGB1. *Il6*, interleukin 6; *Tnfa*, tumor necrosis factor alpha-like; *Il1b*, interleukin-1 beta; *Ifns*, interferon alpha/beta/gamma.

All the three si-HMGB1 RNAs were able to knockdown HMGB1 in the KGN cells (Figure 6N–P). However, si-HMGB1#2 gave a higher knockdown efficiency and so was selected for further experiments ($P < 0.05$; Figure 6N). Western blot and RT-qPCR results showed that the si-HMGB1#2 reduced the protein and mRNA levels of HMGB1, TLR4, TLR9, and NF-κB compared to the si-NC group ($P < 0.05$; Figure 6Q–S).

Taken together, our data demonstrate that the TLR9–MyD88–NF-κB pathway can be suppressed by inhibiting HMGB1 expression.

The p-AKT/t-AKT–GLUT4 pathway participates in the glycometabolism of PCOS mice and KGN cells

In order to explore the detailed mechanism of how HMGB1 inhibition affects glucose metabolism, we assessed the expression of the downstream molecules [39]. The PCOS mice ovaries had lower protein levels of GLUT4 and p-AKT/t-AKT than those of the control group ($P < 0.05$). Glycyrrhizin was able to increase the levels of these proteins in the PCOS mice ($P < 0.05$; Figure 7A). RT-qPCR results (Figure 7B) showed that the PCOS mice had decreased *Glut4*, insulin receptor (*Insr*), and insulin receptor substrate (*Irs*) 1 and 2 mRNA levels compared to the control group ($P < 0.01$, $P < 0.001$, $P < 0.01$, and $P < 0.01$, respectively). After glycyrrhizin treatment, *Insr* level increased significantly ($P < 0.05$). *Glut4* and *Irs2* showed the same trend as *Insr* but the difference was not significant.

Forced HMGB1 expression in the KGN cells decreased the protein levels of GLUT4 and p-AKT/t-AKT; however, this effect was significantly reversed by glycyrrhizin ($P < 0.05$; Figure 7D and E). *Glut4*, *Insr*, and *Irs2* mRNA levels were increased after treating the cells with glycyrrhizin ($P < 0.05$; Figure 7F). HMGB1 knockdown increased the protein levels of GLUT4 and p-AKT/t-AKT ($P < 0.05$; Figure 7G and H). *Glut4* and *Insr* mRNA levels increased after HMGB1 inhibition ($P < 0.05$; Figure 7I).

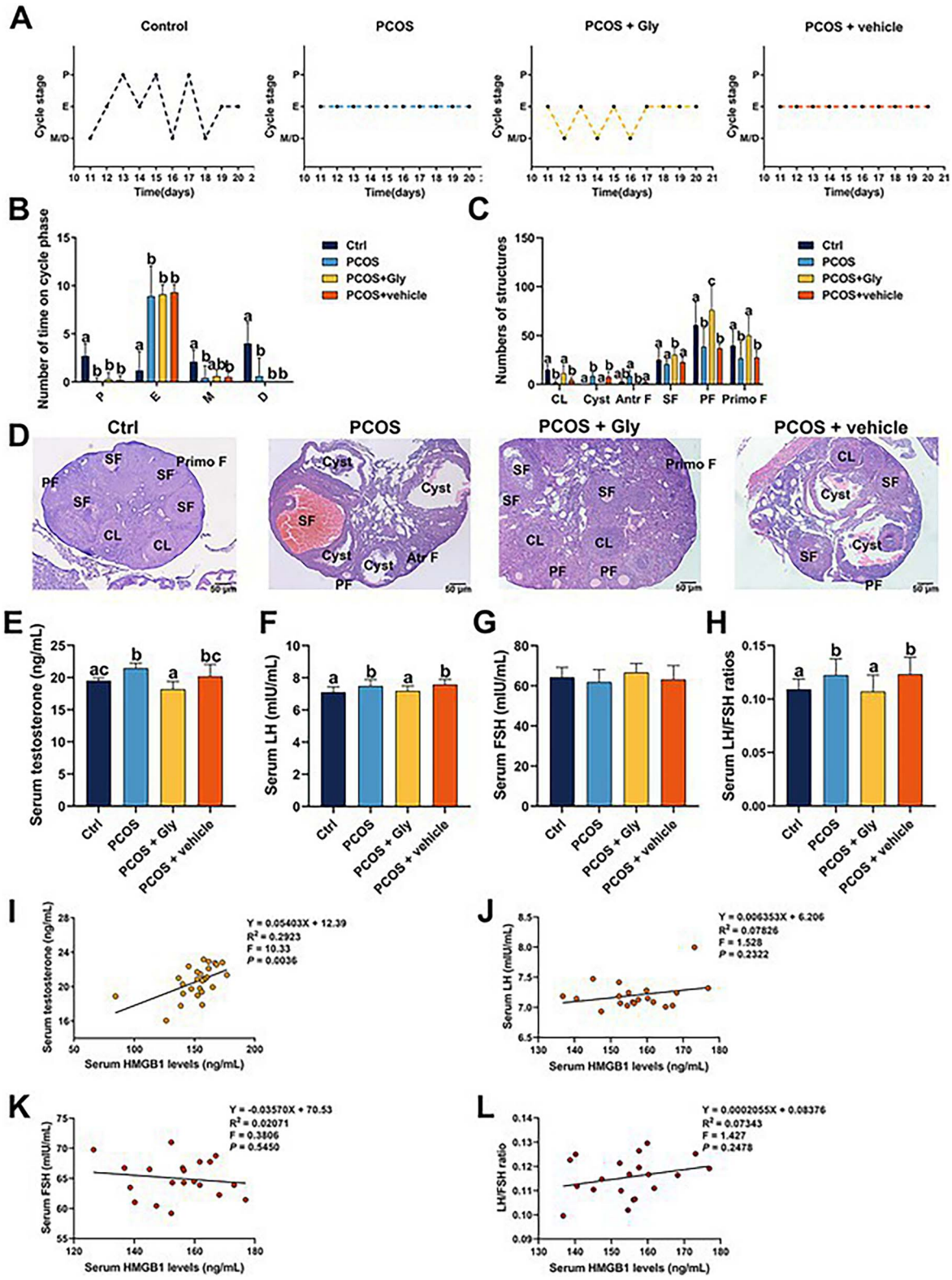

Figure 5. Reproductive manifestations of glycyrrhizin on PCOS mice. (A, B) Representative estrous cycles and corresponding statistics, $n = 5$ per group; (C) H&E images of the mice ovarian sections; (D) Follicles at different developing stages, $n = 6$ per group. (E) Serum testosterone, (F) LH, (G) FSH, (H) LH/FSH ratios ($n = 20$ per group). Correlation between serum HMGB1 level and serum (I) testosterone ($n = 26$), (J) LH, (K) FSH, and (L) LH/FSH ratios from the control and PCOS mice ($n = 20$). The data are expressed as the mean ± SD; different lowercase letters above the columns, such as a, b, and c, indicate $P < 0.05$. If two columns have the same lowercase letter, it indicates no statistical significance. M/D, metestrus/diestrus phase; P, proestrus phase; E, estrus phase; Primo F, primordial follicles; PF, primary follicles; SF, secondary follicles; Atr F, atretic follicles; Cyst, cystic follicles; CL, corpus luteum, LH, luteinizing hormone; FSH, follicle-stimulating hormone.

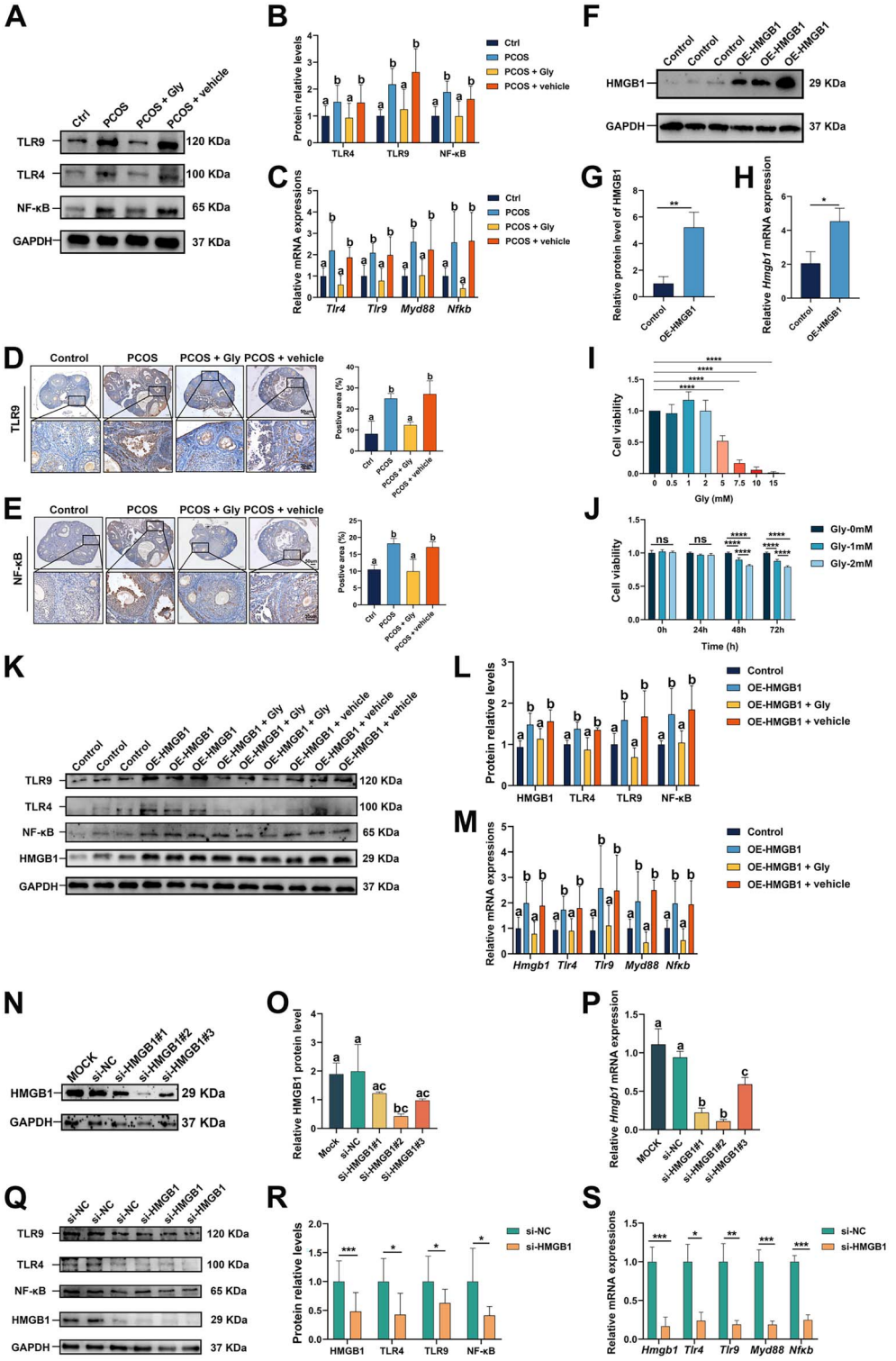

Figure 6. Expressions of TLR9, TLR4, MyD88, and NF-κB on PCOS mice and KGN cells after HMGB1 inhibition. (A, B) The ovarian protein levels of TLR9, TLR4, and NF-κB in the mice ($n = 12$–15 per group) as determined with western blot. (C) Ovarian mRNA levels of *Tlr4*, *Tlr9*, *Myd88*, and *Nfκb* in the mice ($n = 9$–12 per group). Immunohistochemical images of TLR9 (D) and NF-κB (E) in mice ovarian tissues. (F, G) Protein and (H) mRNA levels of HMGB1 in KGN cells transfected with HMGB1 overexpression plasmid, $n = 3$ per group. (I) Cell viability of KGN cells treated with different concentrations of glycyrrhizin for 24 h. (J) Different concentrations of glycyrrhizin were treated for 24, 48, and 72 h for cell viability assays. (K, L) HMGB1, TLR9, TLR4, and NF-κB protein levels after overexpressed HMGB1 *in vitro*, $n = 6$–9 per group. *Hmgb1*, *Tlr4*, *Tlr9*, *Myd88*, and *Nfκb* mRNA levels after overexpression of HMGB1 in vitro ($n = 9$–12 per group). (N, O) Protein and (P) mRNA levels of HMGB1 in KGN cells transfected with different fragments of siRNA, $n = 3$ per group. (Q, R) HMGB1, TLR9, TLR4, and NF-κB protein levels after silencing HMGB1 in vitro, $n = 6$–18 per group. (S) *Hmgb1*, *Tlr4*, *Tlr9*, *Myd88*, and *Nfκb* mRNA levels after inhibiting HMGB1 *in vitro* ($n = 6$–9 per group). Data are presented as mean ± SD. Different lowercase letters above the columns, such as a, b, and c, indicate $P < 0.05$. If two columns have the same lowercase letter, it indicates no statistical significance. $^{*}P < 0.05$, si-NC vs. si-HMGB1; $^{**}P < 0.01$, si-NC vs. si-HMGB1; $^{***}P < 0.001$, si-NC vs. si-HMGB1. HMGB1, high mobility group box 1; TLR4, toll-like receptor 4; TLR9, toll-like receptor 9; MyD88, myeloid differentiation factor 88; NF-κB, nuclear factor kappa-B.

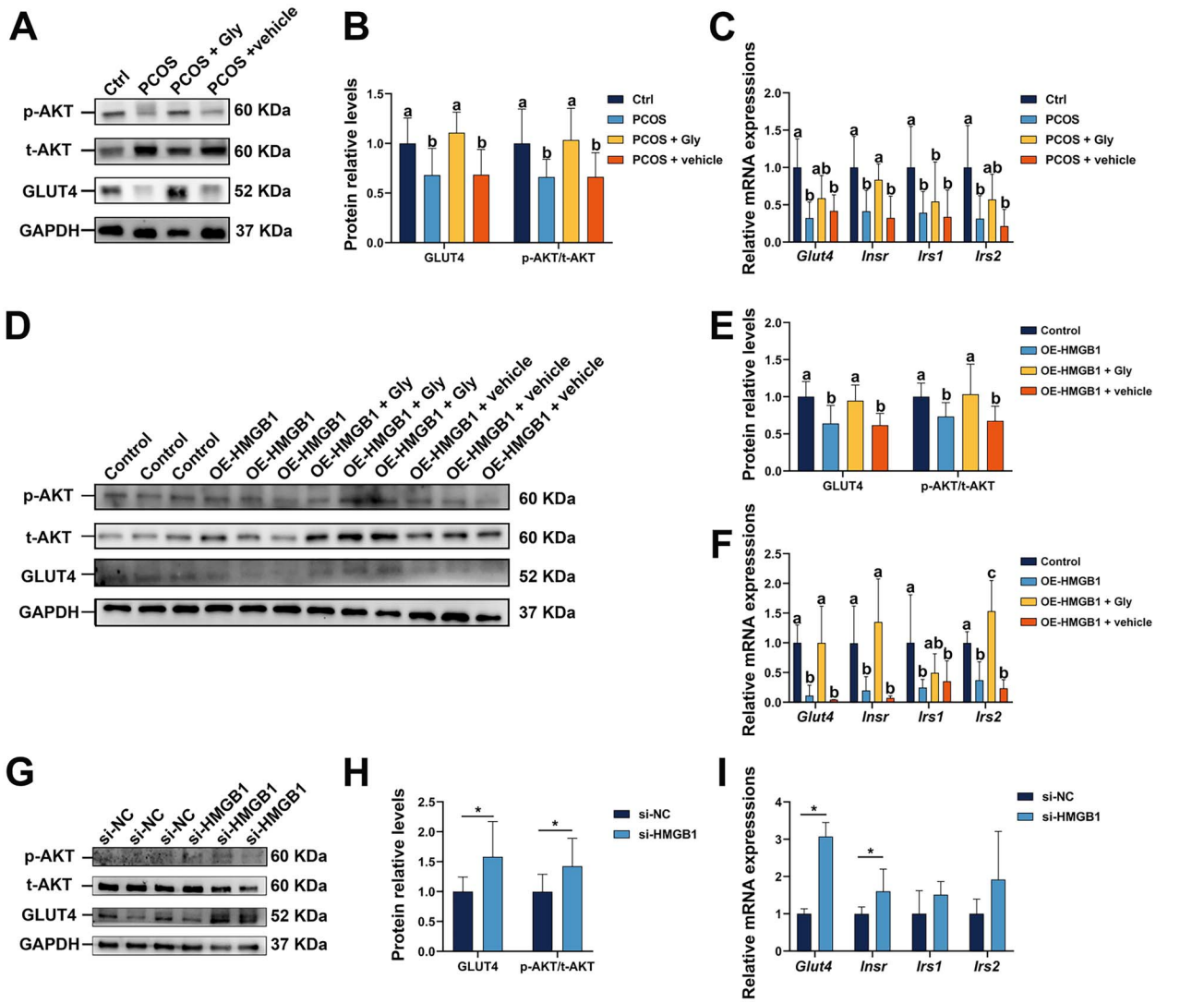

Figure 7. Effects of HMGB1 on the insulin signaling pathway in PCOS mice and KGN cells. (A, B) GLUT4 and p-AKT/t-AKT protein levels and (C) *Glut4*, *Insr*, *Irs1*, and *Irs2* mRNA levels in the mice ovaries ($n = 10$–15 per group). (D, E) The protein levels of GLUT4 and p-AKT/t-AKT and (F) mRNA levels of *Glut4*, *Insr*, *Irs1*, and *Irs2* in the HMGB1-overexpressed and glycyrrhizin management KGN cells ($n = 9$ per group). (G, H) The protein levels of GLUT4 and p-AKT/t-AKT and (I) mRNA levels of *Glut4*, *Insr*, *Irs1*, and *Irs2* in the si-HMGB1 KGN cells ($n = 3$–6 per group). Data are presented as mean ± SD. Different lowercase letters above the columns, such as a, b, and c, indicate $P < 0.05$. If two columns have the same lowercase letter, it indicates no statistical significance; $^{*}P < 0.05$, si-NC vs. si-HMGB1; $^{**}P < 0.01$, si-NC vs. si-HMGB1; $^{***}P < 0.001$, si-NC vs. si-HMGB1. GLUT4, glucose transporter type 4; p-AKT, phosphorylated protein kinase B; INSR, insulin receptor; IRS1, insulin receptor substrate 1; IRS2, insulin receptor substrate 2.

Taken together, our data indicate that the p-AKT/t-AKT–GLUT4 pathway can be activated by inhibiting HMGB1 expression.

Discussion

Several studies, including this study (Figure 8), have confirmed that the serum level of HMGB1 is higher in PCOS [18], suggesting that inhibiting HMGB1 could be a reliable therapeutic approach against PCOS. Glycyrrhizin, a drug believed to be safe for human use, can directly bind to and inhibit HMGB1 [40]. Although glycyrrhizin has shown potential benefits in the treatment of cancer, inflammation, and obesity [20, 21], whether and how it can help in treating PCOS has not been reported.

In this study, we initially confirmed that glycyrrhizin effectively reduces HMGB1 levels in the serum and ovarian tissues of PCOS mice. Then, we assessed the therapeutic impacts of glycyrrhizin on the PCOS mice. Glycyrrhizin could revert metabolic disorders in the PCOS mice. The PCOS mice had higher fasting glucose and insulin levels (a predictor of insulin resistance), but this was reversed by glycyrrhizin. Moreover, our OGTT and ITT data revealed that glycyrrhizin treatment counteracted the delayed glucose tolerance and the increased AUC in the PCOS mice. In addition, after the glycyrrhizin-induced HMGB1 inhibition, HOMA-IR index decreased while HOMA-β index increased. This indicates that glycyrrhizin alleviated impaired glucose metabolism and β-cell dysfunction to counteract insulin resistance in the PCOS mice. For lipid metabolism, we found that serum LDL-C significantly increased in PCOS and was positively correlated with serum HMGB1. Unfortunately, glycyrrhizin could not significantly improve lipid metabolism, and this may be due to the small sample size.

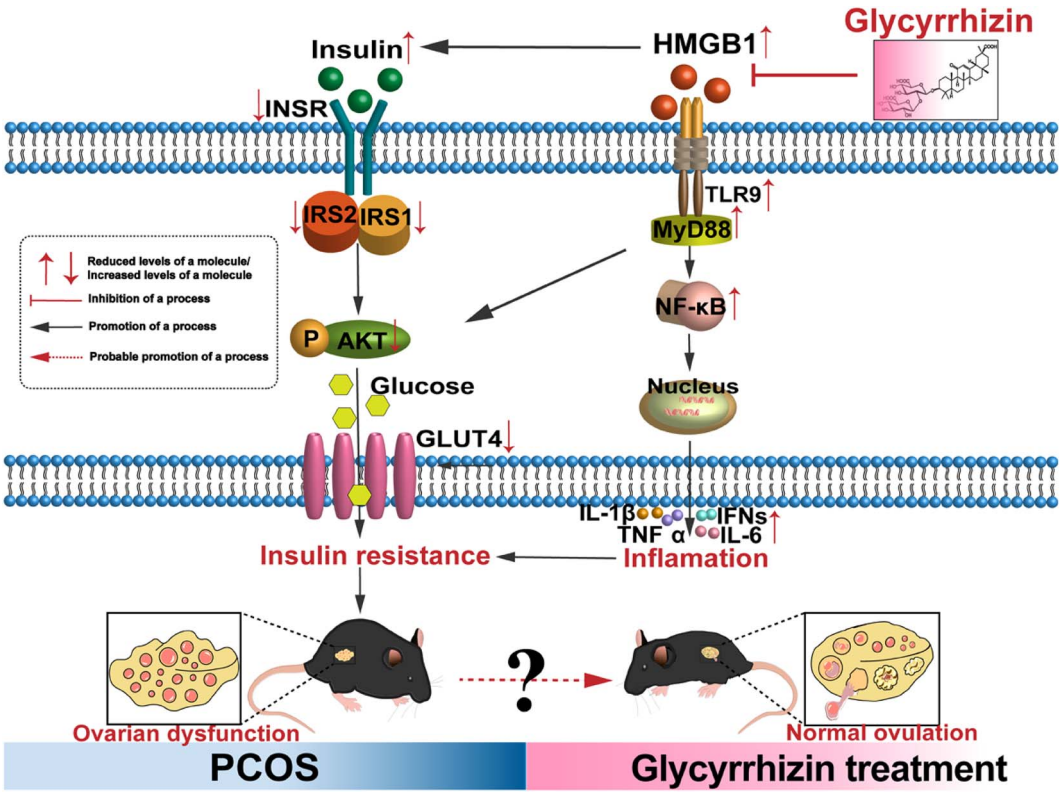

Figure 8. Proposed mechanism of how glycyrrhizin counteracts the pathophysiology of PCOS. During PCOS, ovarian GLUT4 is downregulated and that weakens intracellular glucose uptake. Also, reduced ovarian INSR expression leads to higher insulin levels and insulin resistance. These lead to excessive glucose storage and eventual weight gain. Upregulation of ovarian HMGB1 amplifies the MyD88 cascade, via the activation TLR9, to target NF-κB. This aggravates the inflammatory responses and eventually lead to chronic low-grade inflammation. The interplay of all these factors consequently results in ovulatory dysfunction in PCOS. When PCOS mice are treated with glycyrrhizin, it reverses the weight gain, chronic low-grade inflammation, and insulin resistance by inhibiting the HMGB1–TLR9–MyD88–NF-κB pathway and by activating the p-AKT/t-AKT–GLUT4 signaling pathway. This causes the PCOS mice to ovulate at regular intervals. HMGB1, high mobility group box 1; TLR9, toll-like receptor 9; MyD88, myeloid differentiation factor 88; NF-κB, nuclear factor kappa-B; INSR, insulin receptor; IRS1/2, insulin receptor substrate 1/2; p-AKT, phosphorylated protein kinase B; GLUT4, glucose transporter type 4; IL-6, interleukin 6; TNFα, tumor necrosis factor alpha; IL-1β, interleukin 1 beta; IFNs, interferon alpha/beta/gamma.

Furthermore, regarding ovarian function, we found that glycyrrhizin prevented an increase in the number of cystic follicles and decrease in the number of the corpus lutea and prolonged the metestrus phase time in the PCOS mice. It is worth noting that the serum testosterone, LH, and LH/FSH ratios were improved by glycyrrhizin, with the serum testosterone having a significant positive correlation with HMGB1 levels. Since it has been reported that HMGB1 participates in the development of insulin resistance [41], our current findings suggest that glycyrrhizin prevented DHEA plus HFD-induced PCOS development. We explored the molecular mechanism of how glycyrrhizin affects glucose metabolism and ovarian functions in the PCOS mice. We found that the decreased expression of INSR (an essential component of the insulin signaling pathway) in the PCOS mice could be reversed by glycyrrhizin. Also, HMGB1 knockdown led to an increase in INSR expression. Interestingly, neither glycyrrhizin treatment nor HMGB1 knockdown could have a significant recovery effect on the expression of the cytoplasmic signaling adapter proteins: IRS1 and IRS2. This may be due to the small sample size we used in this study.

The p-AKT/t-AKT–GLUT4 signaling pathway has been shown to be involved in insulin resistance [42]. The dysregulation of AKT results in insulin resistance [43]. MyD88 also participants in adiposity and insulin resistance in female mice [44] and can be conjugated directly to AKT [45]. GLUT4 plays a vital role in cellular glucose balance. A lower level of GLUT4 is evident in PCOS patients with obesity [46]. We found that the decreased expression of GLUT4 and p-AKT in PCOS could be reversed by glycyrrhizin, which implies that glycyrrhizin could improve insulin resistance in PCOS through promoting AKT phosphorylation and facilitating GLUT4 expression to help transport glucose by inhibiting HMGB1. Treatment with glycyrrhizin reversed the HMGB1-induced decrease in GLUT4, p-AKT, and INSR in HMGB1 overexpression KGN cells. Silencing of HMGB1 yielded a similar effect.

Several studies have indicated that chronic low-grade inflammation promotes insulin resistance [12, 47]. We found that the swollen uteri of the PCOS mice were alleviated by glycyrrhizin. This occurrence may relate to inflammation. Tumor necrosis factor alpha (TNFα) and interleukin (IL)-6 have been reported to exert regulatory effects on ovarian steroidogenesis [48]. Interferon alpha (IFN α) and IFN β are involved in most chronic viral immune pathogenesis [49]. It has been found that elevated expression of IFN γ increased the pyroptosis of macrophages and exacerbated its effect on the estrogen receptor in granular cells [50]. In this current study, we found that the increased mRNA levels of *Il6*, *Tnfa*, *Ifna*, *Ifnb1*, and *Ifng* in the PCOS mice were decreased after

glycyrrhizin administration. In vitro glycyrrhizin treatment decreased the mRNA levels of *Il6*, *Tnfa*, *Ifna*, and *Ifnb1* in the HMGB1-overexpression cells, and silencing of HMGB1 significantly decreased the mRNA levels of *Il6*, *Tnfa*, and *Ifnb1*; this is consistent with the in vivo results. This indicates that glycyrrhizin exhibits a significant anti-inflammatory effect on PCOS.

To further investigate the mechanism of how glycyrrhizin exhibits anti-inflammatory effects in PCOS mice, we investigated the downstream targets of HMGB1. It is known that extracellular HMGB1 transmits signals into cells by interacting with the receptor for advanced glycation end products and TLR-2/4/9 [36]. TLR4 is one of the classical receptors involved in HMGB1 binding. It has been reported that cryptotanshinone can prevent PCOS ovarian damage through the HMGB1/TLR4 pathway [51]. We also found that TLR4 was elevated in the PCOS mice. TLR9 has also been found to regulate adipose tissue inflammation and obesity-related metabolic disorders [52]. After HMGB1 has bound to TLR9, a mechanism is transduced through MyD88 [53]. MyD88 promotes insulin resistance by binding to AKT. It can also activate the NF-κB signaling pathway [45]. However, this mechanism has not been reported in PCOS. Our results show that the increased expressions of TLR4, TLR9, MyD88, NF-κB, and other inflammatory factors could be reduced via the inhibition of HMGB1, both in vivo and in vitro. Hence, we suggest that glycyrrhizin exerts its anti-inflammatory effects on PCOS mice by possibly suppressing the TLR9–MyD88–NF-κB signaling pathway.

Conclusion

Glycyrrhizin exhibits beneficial effects against inflammation, insulin resistance, and ovarian dysfunction in PCOS via preventing or, at least, thwarting DHEA/HFD-induced PCOS development. However, further studies are needed to verify its efficacy in PCOS patients.

Acknowledgment

We thank Sadaf Pervaz, Armin Czika, Xiang-Lu Wu, and Ming-Xing Chen for their assistance in tissue processing. We thank Xue-Mei Chen and Fang-Fang Li for their experimental support.

Supplementary material

Supplementary material is available at *BIOLRE* online.

Conflict of Interest: The authors have declared that no conflict of interest exists.

Authors' contributions

YW, MW, and YD conceived the research idea and designed the experiments. JY, UA, YS, and OA validated the conception. JY carried out the experiments. JY analyzed the data and wrote the manuscript. MW and YD wrote the review and edited the manuscript. EAA-G, QF, YW, MW, and YD revised the manuscript. Financial support was provided from YW, MW, and YD. All authors listed have made a substantial, direct, and intellectual contribution to the work and approved it for publication.

Data availability

The data underlying this article will be shared on reasonable request to the corresponding author.

References

1. Teede HJ, Misso ML, Costello MF, Dokras A, Laven J, Moran L, Piltonen T, Norman RJ, International PCOS Network, Andersen M, Azziz R, Balen A, *et al*. Recommendations from the international evidence-based guideline for the assessment and management of polycystic ovary syndrome. *Hum Reprod* 2018; **33**: 1602–1618.
2. McCartney CR, Marshall JC. CLINICAL PRACTICE. Polycystic ovary syndrome. *N Engl J Med* 2016; **375**:54–64.
3. Norman RJ, Dewailly D, Legro RS, Hickey TE. Polycystic ovary syndrome. *Lancet* 2007; **370**:685–697.
4. Teede H, Deeks A, Moran L. Polycystic ovary syndrome: a complex condition with psychological, reproductive and metabolic manifestations that impacts on health across the lifespan. *BMC Med* 2010; **8**:41.
5. Rudnicka E, Suchta K, Grymowicz M, Calik-Ksepka A, Smolarczyk K, Duszewska AM, Smolarczyk R, Meczekalski B. Chronic low grade inflammation in pathogenesis of PCOS. *Int J Mol Sci* 2021; **22**:3789.
6. Cussons AJ, Stuckey BG, Watts GF. Metabolic syndrome and cardiometabolic risk in PCOS. *Curr Diab Rep* 2007; **7**:66–73.
7. Marshall JC, Dunaif A. Should all women with PCOS be treated for insulin resistance? *Fertil Steril* 2012; **97**:18–22.
8. Joham AE, Teede HJ, Hutchison SK, Stepto NK, Harrison CL, Strauss BJ, Paul E, Watt MJ. Pigment epithelium-derived factor, insulin sensitivity, and adiposity in polycystic ovary syndrome: impact of exercise training. *Obesity (Silver Spring)* 2012; **20**: 2390–2396.
9. Valsamakis G, Lois K, Kumar S, Mastorakos G. Metabolic and other effects of pioglitazone as an add-on therapy to metformin in the treatment of polycystic ovary syndrome (PCOS). *Hormones (Athens)* 2013; **12**:363–378.
10. Guo R, Zheng Y, Yang J, Zheng N. Association of TNF-alpha, IL-6 and IL-1beta gene polymorphisms with polycystic ovary syndrome: a meta-analysis. *BMC Genet* 2015; **16**:5.
11. Zhang Y, Che L, Zhang M, He J. Common cytokine polymorphisms and predisposition to polycystic ovary syndrome: a meta-analysis. *Endocr J* 2020; **67**:561–567.
12. Li C, Xing C, Zhang J, Zhao H, Shi W, He B. Eight-hour time-restricted feeding improves endocrine and metabolic profiles in women with anovulatory polycystic ovary syndrome. *J Transl Med* 2021; **19**:148.
13. Peecher DL, Binder AK, Gabriel KI. Rodent models of mental illness in polycystic ovary syndrome: the potential role of hypothalamic-pituitary-adrenal dysregulation and lessons for behavioral researchers. *Biol Reprod* 2019; **100**:590–600.
14. Ni XR, Sun ZJ, Hu GH, Wang RH. High concentration of insulin promotes apoptosis of primary cultured rat ovarian granulosa cells via its increase in extracellular HMGB1. *Reprod Sci* 2015; **22**: 271–277.
15. Plazyo O, Romero R, Unkel R, Balancio A, Mial TN, Xu Y, Dong Z, Hassan SS, Gomez-Lopez N. HMGB1 induces an inflammatory response in the chorioamniotic membranes that is partially mediated by the inflammasome. *Biol Reprod* 2016; **95**:130.
16. Bao GQ, He L, Lee D, D'Angelo J, Wang HC. An ongoing search for potential targets and therapies for lethal sepsis. *Mil Med Res* 2015; **2**:20.
17. Gentile LF, Moldawer LL. HMGB1 as a therapeutic target for sepsis: it's all in the timing! *Expert Opin Ther Targets* 2014; **18**: 243–245.
18. Wang HH, Lin M, Xiang GD. Serum HMGB1 levels and its association with endothelial dysfunction in patients with polycystic ovary syndrome. *Physiol Res* 2018; **67**:911–919.

19. Zhu HL, Chen YQ, Zhang ZF. Downregulation of lncRNA ZFAS1 and upregulation of microRNA-129 repress endocrine disturbance, increase proliferation and inhibit apoptosis of ovarian granulosa cells in polycystic ovarian syndrome by downregulating HMGB1. *Genomics* 2020; **112**:3597–3608.
20. Khaksa G, Zolfaghari ME, Dehpour AR, Samadian T. Anti-inflammatory and anti-nociceptive activity of disodium glycyrrhetinic acid hemiphthalate. *Planta Med* 1996; **62**:326–328.
21. Eu CH, Lim WY, Ton SH, bin Abdul Kadir K. Glycyrrhizic acid improved lipoprotein lipase expression, insulin sensitivity, serum lipid and lipid deposition in high-fat diet-induced obese rats. *Lipids Health Dis* 2010; **9**:81.
22. Velez LM, Seldin M, Motta AB. Inflammation and reproductive function in women with polycystic ovary syndrome†. *Biol Reprod* 2021; **104**:1205–1217.
23. Lai H, Jia X, Yu Q, Zhang C, Qiao J, Guan Y, Kang J. High-fat diet induces significant metabolic disorders in a mouse model of polycystic ovary syndrome. *Biol Reprod* 2014; **91**:127.
24. Wang M, Zhao D, Xu L, Guo W, Nie L, Lei Y, Long Y, Liu M, Wang Y, Zhang X, Zhang L, Li H, *et al*. Role of PCSK9 in lipid metabolic disorders and ovarian dysfunction in polycystic ovary syndrome. *Metabolism* 2019; **94**:47–58.
25. Su YN, Wang MJ, Yang JP, Wu XL, Xia M, Bao MH, Ding YB, Feng Q, Fu LJ. Effects of Yulin Tong Bu formula on modulating gut microbiota and fecal metabolite interactions in mice with polycystic ovary syndrome. *Front Endocrinol (Lausanne)* 2023; **14**:1122709.
26. Dai M, Xiao R, Cai L, Ge T, Zhu L, Hu Q. HMGB1 is mechanistically essential in the development of experimental pulmonary hypertension. *Am J Physiol Cell Physiol* 2019; **316**:C175–c185.
27. Feng W, Wang J, Yan X, Zhang Q, Chai L, Wang Q, Shi W, Chen Y, Liu J, Qu Z, Li S, Xie X, *et al*. ERK/Drp1-dependent mitochondrial fission contributes to HMGB1-induced autophagy in pulmonary arterial hypertension. *Cell Prolif* 2021; **54**:e13048.
28. Ngo HT, Hetland RB, Sabaredzovic A, Haug LS, Steffensen IL. In utero exposure to perfluorooctanoate (PFOA) or perfluorooctane sulfonate (PFOS) did not increase body weight or intestinal tumorigenesis in multiple intestinal neoplasia (min/+) mice. *Environ Res* 2014; **132**:251–263.
29. Brennan-Speranza TC, Henneicke H, Gasparini SJ, Blankenstein KI, Heinevetter U, Cogger VC, Svistounov D, Zhang Y, Cooney GJ, Buttgereit F, Dunstan CR, Gundberg C, *et al*. Osteoblasts mediate the adverse effects of glucocorticoids on fuel metabolism. *J Clin Invest* 2012; **122**:4172–4189.
30. Lundbaek K. Intravenous glucose tolerance as a tool in definition and diagnosis of diabetes mellitus. *Br Med J* 1962; **1**:1507–1513.
31. Liu M, Zhang D, Zhou X, Duan J, Hu Y, Zhang W, Liu Q, Xu B, Zhang A. Cell-free fat extract improves ovarian function and fertility in mice with premature ovarian insufficiency. *Stem Cell Res Ther* 2022; **13**:320.
32. Myers M, Britt KL, Wreford NG, Ebling FJ, Kerr JB. Methods for quantifying follicular numbers within the mouse ovary. *Reproduction* 2004; **127**:569–580.
33. Nishi Y, Yanase T, Mu Y, Oba K, Ichino I, Saito M, Nomura M, Mukasa C, Okabe T, Goto K, Takayanagi R, Kashimura Y, *et al*. Establishment and characterization of a steroidogenic human granulosa-like tumor cell line, KGN, that expresses functional follicle-stimulating hormone receptor. *Endocrinology* 2001; **142**:437–445.
34. Zheng Q, Li Y, Zhang D, Cui X, Dai K, Yang Y, Liu S, Tan J, Yan Q. ANP promotes proliferation and inhibits apoptosis of ovarian granulosa cells by NPRA/PGRMC1/EGFR complex and improves ovary functions of PCOS rats. *Cell Death Dis* 2017; **8**:e3145.
35. Zhang Q, Ren J, Wang F, Pan M, Cui L, Li M, Qu F. Mitochondrial and glucose metabolic dysfunctions in granulosa cells induce impaired oocytes of polycystic ovary syndrome through Sirtuin 3. *Free Radic Biol Med* 2022; **187**:1–16.
36. Paudel YN, Angelopoulou E, Piperi C, Balasubramaniam V, Othman I, Shaikh MF. Enlightening the role of high mobility group box 1 (HMGB1) in inflammation: updates on receptor signalling. *Eur J Pharmacol* 2019; **858**:172487.
37. Gu BX, Wang X, Yin BL, Guo HB, Zhang HL, Zhang SD, Zhang CL. Abnormal expression of TLRs may play a role in lower embryo quality of women with polycystic ovary syndrome. *Syst Biol Reprod Med* 2016; **62**:353–358.
38. Medzhitov R, Preston-Hurlburt P, Kopp E, Stadlen A, Chen C, Ghosh S, Janeway CA Jr. MyD88 is an adaptor protein in the hToll/IL-1 receptor family signaling pathways. *Mol Cell* 1998; **2**:253–258.
39. Zhang C, Hu J, Wang W, Sun Y, Sun K. HMGB1-induced aberrant autophagy contributes to insulin resistance in granulosa cells in PCOS. *FASEB J* 2020; **34**:9563–9574.
40. Girard JP. A direct inhibitor of HMGB1 cytokine. *Chem Biol* 2007; **14**:345–347.
41. Cirillo F, Catellani C, Lazzeroni P, Sartori C, Tridenti G, Vezzani C, Fulghesu AM, Madeddu E, Amarri S, Street ME. HMGB1 is increased in adolescents with polycystic ovary syndrome (PCOS) and decreases after treatment with MYO-inositol (MYO) in combination with alpha-lipoic acid (ALA). *Gynecol Endocrinol* 2020; **36**:588–593.
42. Huang JP, Huang SS, Deng JY, Hung LM. Impairment of insulin-stimulated Akt/GLUT4 signaling is associated with cardiac contractile dysfunction and aggravates I/R injury in STZ-diabetic rats. *J Biomed Sci* 2009; **16**:77.
43. Goldbraikh D, Neufeld D, Eid-Mutlak Y, Lasry I, Gilda JE, Parnis A, Cohen S. USP1 deubiquitinates Akt to inhibit PI3K-Akt-FoxO signaling in muscle during prolonged starvation. *EMBO Rep* 2020; **21**:e48791.
44. Mahmassani ZS, Reidy PT, McKenzie AI, Petrocelli JJ, Matthews O, de Hart NM, Ferrara PJ, O'Connell RM, Funai K, Drummond MJ. Absence of MyD88 from skeletal muscle protects female mice from inactivity-induced adiposity and insulin resistance. *Obesity (Silver Spring)* 2020; **28**:772–782.
45. Lu X, He Y, Tang C, Wang X, Que L, Zhu G, Liu L, Ha T, Chen Q, Li C, Xu Y, Li J, *et al*. Triad3A attenuates pathological cardiac hypertrophy involving the augmentation of ubiquitination-mediated degradation of TLR4 and TLR9. *Basic Res Cardiol* 2020; **115**:19.
46. Zhang N, Liu X, Zhuang L, Liu X, Zhao H, Shan Y, Liu Z, Li F, Wang Y, Fang J. Berberine decreases insulin resistance in a PCOS rats by improving GLUT4: dual regulation of the PI3K/AKT and MAPK pathways. *Regul Toxicol Pharmacol* 2020; **110**:104544.
47. Xu H, Barnes GT, Yang Q, Tan G, Yang D, Chou CJ, Sole J, Nichols A, Ross JS, Tartaglia LA, Chen H. Chronic inflammation in fat plays a crucial role in the development of obesity-related insulin resistance. *J Clin Invest* 2003; **112**:1821–1830.
48. Samir M, Glister C, Mattar D, Laird M, Knight PG. Follicular expression of pro-inflammatory cytokines tumour necrosis factor-α (TNFα), interleukin 6 (IL6) and their receptors in cattle: TNFα, IL6 and macrophages suppress thecal androgen production in vitro. *Reproduction* 2017; **154**:35–49.
49. Tian Y, Jennings J, Gong Y, Sang Y. Viral infections and interferons in the development of obesity. *Biomolecules* 2019; **9**:726.
50. Huang J, Chen P, Xiang Y, Liang Q, Wu T, Liu J, Zeng Y, Zeng H, Liang X, Zhou C. Gut microbiota dysbiosis-derived macrophage pyroptosis causes polycystic ovary syndrome via steroidogenesis disturbance and apoptosis of granulosa cells. *Int Immunopharmacol* 2022; **107**:108717.
51. Yang Y, Yang L, Qi C, Hu G, Wang L, Sun Z, Ni X. Cryptotanshinone alleviates polycystic ovary syndrome in rats by regulating the HMGB1/TLR4/NF-κB signaling pathway. *Mol Med Rep* 2020; **22**:3851–3861.
52. Hong CP, Yun CH, Lee GW, Park A, Kim YM, Jang MH. TLR9 regulates adipose tissue inflammation and obesity-related metabolic disorders. *Obesity (Silver Spring)* 2015; **23**:2199–2206.
53. Green NM, Marshak-Rothstein A. Toll-like receptor driven B cell activation in the induction of systemic autoimmunity. *Semin Immunol* 2011; **23**:106–112.